Environ Sci Pollut Res (2018) 25:10362–10370
DOI 10.1007/s11356-017-9367-9



# An enhancement of antimicrobial efficacy of biogenic and ceftriaxone-conjugated silver nanoparticles: green approach

**Rajasree Shanmuganathan[1] · Davoodbasha MubarakAli[2] · Desika Prabakar[3] · Harshiny Muthukumar[4] · Nooruddin Thajuddin[2] · Smita S. Kumar[5] · Arivalagan Pugazhendhi[6]**

Received: 6 April 2017 / Accepted: 23 May 2017 / Published online: 9 June 2017


**Abstract** Of the various methods explored for the synthesis of nanoparticles, biogenesis of silver nanoparticles (AgNPs) received great attention due to their versatile properties. In this report, *Daucus carota* extract was used for the synthesis of AgNPs and ceftriaxone was conjugated with AgNPs to enhance their antimicrobial efficacy. The conjugated and unconjugated AgNPs were characterized by adopting UV-Vis spectroscopy, FTIR, AFM, DLS, and TEM, which revealed the SPR peak at 420 nm and spherical shaped nanoparticles of 20 nm size, respectively. The antimicrobial efficacies of the unconjugated AgNPs and ceftriaxone-conjugated AgNPs were tested against ceftriaxone-resistant human pathogens, *Bacillus cereus*, *Staphylococcus aureus*, *Klebsiella pneumoniae*, and *Pseudomonas aeruginosa*. The ceftriaxone-conjugated AgNPs showed high inhibitory action (23 mm) than the unconjugated AgNPs (18 mm) at the concentration of 50 μg/mL. Both the unconjugated and ceftriaxone-conjugated AgNPs were found to be non-toxic on EAC cells at 50 μg/mL. The dose-dependent cytotoxic activities were observed on increasing the concentration of the AgNPs. The ceftriaxone-conjugated AgNPs showed high activity than the unconjugated AgNPs. The enhanced activity could be useful to treat ceftriaxone-resistant human pathogens.

**Keywords** Biogenesis · AgNPs · Ceftriaxone · Antimicrobials · Cytotoxic

Responsible editor: Philippe Garrigues

✉ Arivalagan Pugazhendhi
arivalagan.pugazhendhi@tdt.edu.vn

[1] CoRx Life sciences and Pharmaceutical (CLAP) Private Limited, Tiruchirappalli, Tamil Nadu 620 020, India

[2] National Repository for Microalgae and Cyanobacteria - Freshwater (DBT), Department of Microbiology, Bharathidasan University, Tiruchirappalli, Tamil Nadu 620 024, India

[3] Anna University, ACT Campus, Chennai, Tamil Nadu 25, India

[4] Department of Biotechnology, Periyar Maniammai University, Thanjavur, Tamil Nadu 613 403, India

[5] Department of Environmental Science and Engineering, Guru Jambheshwar University of Science and Technology, Hisar, Haryana 125001, India

[6] Green Processing, Bioremediation and Alternative Energies Research Group (GPBAE), Faculty of Environment and Labour Safety, Ton Duc Thang University, Ho Chi Minh City, Vietnam

## Introduction

Heeding towards the attainment of extreme specificity and an increased efficiency in various arenas of research, the drift towards the nanoscale poses as the ideal weapon of recent times. Moreover, the continuous increase in multidrug-resistant microbes and relative unavailability of medicine together with the emergence of adverse side effects of certain antibiotics has warranted the discovery of new drugs, which addresses these issues.

Nanoparticles have attracted considerable attention of the scientific community on account of their unique functional characteristics coupled with tunable hydrophilic-hydrophobic balance and their exceptional abilities for target-specific localization and others (Salem et al. 2016; Shankar et al. 2016). Particularly, silver nanoparticles (AgNPs) have conquered extreme interest, owing to their beneficial characteristics of antimicrobial, antioxidant, and antitumor activities, which aid in the development of pharmaceutical drugs. (Ramkumar et al. 2017; Saratale et al. 2017; Vijayan et al. 2016). The applications of AgNPs have also been successfully applied to food industries, textile industries, and agriculture (Gomaa 2017; Maráková et al. 2017; Ostaszewska

et al. 2016). A number of different approaches have been widely used for the synthesis of AgNPs reported in the literature, namely, chemical reduction, photoreduction, reverse micelle, solution plasma, thermal decomposition, ultrasonication, microwave irradiation, and electrochemical methods (Venugopal et al. 2017; MubarakAli et al. 2016; Muthu and Priya 2017). However, for the past few decades, various rapid chemical methods have been replaced by green synthesis in the view of avoiding toxicity of the process and increasing productivity. For instance, a facial method has been applied to the reduction of Ag ions to AgNPs through plant leaf extract (MubarakAli et al. 2011). In a much broader perspective, Venugopal et al. (2017) reported the synthesis of AgNPs using crude extract of *Syzygium aromaticum* and studied the anticancer activity against MCF 7 and A549 cells, which cause breast and lung cancers, respectively. Su et al. (2017) and Liu et al. (2013) reported that the toxicity effects of AgNPs covered a wider range of pathogenic bacteria, both gram positive (*Staphylococcus aureus*, *Bacillus subtilis*) and gram negative (*Escherichia coli*), and yeast (*Candida albicans*).

In view of delving further, the drug ceftriaxone is a third-generation cephalosporin antibiotic with a broad spectrum activity against gram-positive and gram-negative bacteria. However, ceftriaxone does not show complete efficacy against a wide range of pathogenic bacteria. In this respect, the incorporation of AgNPs, owing to their exceptional chemical, physical, and photophysical properties, might mitigate the issue at hand, enabling targeted and controlled delivery of drugs (Harshiny et al. 2015; Iravani et al. 2014). Predominantly, modification of the surface of AgNPs has facilitated the binding of drugs to a great extent. However, direct conjugation also provides promising results as it is explicit from the analysis of treatment of bacterial infections, utilizing conjugates of metal nanoparticles with antibiotics (Sperling and Parak 2010). Several researchers have proved that the green chemistry approach is an eco-friendly, cost-effective, and efficient method for the synthesis of AgNPs (Pugazhendhi et al. 2015; Ramkumar et al. 2017).

In this context, the present study has reported the synthesis and characterization of AgNPs using *Daucus carota* extract, which were then conjugated with ceftriaxone. The synthesized compounds were evaluated for antibacterial activity. AgNPs were biosynthesized using the extract of *D. carota*, which is a readily available root vegetable mainly used for herbal preparations with high quantities of alpha- and beta-carotene, and is a good source of vitamin K and vitamin B6, which aids in thrombosis and neurogenesis. Yet, the novelty of our study lies on the fact that the conjugation of biogenic AgNPs with ceftriaxone contributes a distinctive approach for achieving superior antibacterial effects compared to both ceftriaxone and unconjugated AgNPs. Hence, the exploration of biological sources for the synthesis of nanoparticles would not only dial down the concerns but also attain an economical high as well. One such approach has been briefed in this paper reporting the use of *D. carota* for synthesis of AgNPs. Moreover, the excessive use of antimicrobial agents and its ultimate contribution to the emergence of antibiotic resistant strains demand the discovery of alternative forms of drugs.

## Materials and methods

### Preparation of carrot extract

Fresh carrot, *D. carota*, was purchased from a local market in Tiruchirappalli, India. Initially, collected samples were washed thoroughly with double distilled water to remove unwanted adhering debris. Secondly, 10 g of *D. carota* was chopped into small-size pieces and boiled with sterile deionized water for 10–15 min and then kept in an extractor for 5 min. The obtained extract was centrifuged at 10000 rpm for 5 min and filtered through Whatman No.1 filter paper. Finally, the resultant filtrate was used for AgNP synthesis and the filtrate was stored in a refrigerator (4 °C) for further use.

### Optimization of synthesis of AgNPs

Biogenic AgNPs were prepared using the high purity commercial grade silver nitrate ($AgNO_3$, Sigma-Aldrich, USA). In a typical reaction procedure, 1 mM of $AgNO_3$ was prepared in 90 mL of sterile deionized water, and 10 mL of *D. carota* extract was added simultaneously and stirred continuously at room temperature. The color change was observed after the addition of *D. carota* extract (Fig. 1) (Pugazhendhi et al. 2016). For the optimization of efficient AgNP synthesis, critical factors such as pH (6–9), temperature (25–60 °C), and concentration of $AgNO_3$ (1–5 mM) were tested at various ranges.

### Synthesis of ceftriaxone-AgNP conjugates

Conjugation of ceftriaxone with AgNPs was performed by adopting the method previously reported (Harshiny et al. 2015). Briefly, equal volumes of both $AgNO_3$ and ceftriaxone were prepared in deionized water and the solutions were mixed in the 8:1 M ratio of AgNPs and ceftriaxone, respectively, for conjugation. Then, the mixture was kept in a rotary shaker for 24 h at 200 rpm, and the resulting product was centrifuged at 10,000 rpm for 10 min. Finally, the ceftriaxone-conjugated AgNPs were freeze dried and stored at 4 °C for further characterization.

### Characterization studies

The absorption spectra of AgNPs synthesized using *D. carota* was obtained using UV-visible spectroscopy (UV-1800, Shimadzu, Japan), scanned over an interval ranging from

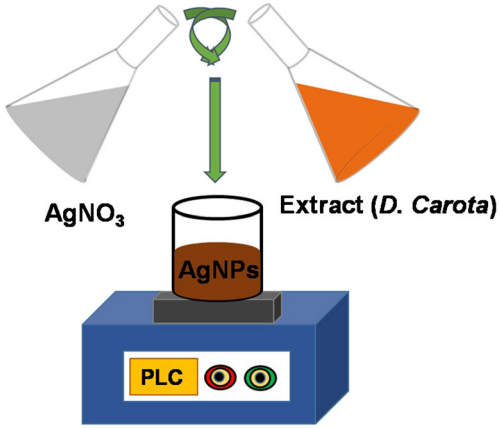


**Fig. 1** Schematic diagram of synthesis of silver nanoparticles (AgNPs)

300 to 800 nm. Absorption spectra were obtained for all the parameters (pH, temperature, and incubation time) tested for the effective synthesis of AgNPs. Fourier transform infrared spectroscopy was performed to confirm the presence of possible functional groups responsible for reduction and capping behavior of biomolecules present in the *D. carota* extract. Fourier transform infrared (FTIR: iS5, Nicolet Thermo, USA) spectra of the biogenic AgNPs were recorded over a spectral range of 400–4000 $cm^{-1}$ using KBr pellets operated with a resolution of 4 $cm^{-1}$. To determine the crystalline structure of biogenic AgNPs conjugated with ceftriaxone, X-ray diffraction patterns (XRD: X′Pert PRO, Japan) were acquired with X′Pert High Score Plus software operating at a voltage of 45 kV and a current of 40 mA with Cu Kα radiation. Size, stability, and distribution of AgNPs were analyzed by zeta potential and particle size analyzer (PSA: Malvern, UK). The topography of the ceftriaxone-conjugated biogenic AgNPs was investigated using atomic force microscopy (AFM: Veeco Innova, Bruker, USA) having a silicon nitride tip at range of 25–30 mm, and the images were analyzed using SPM lab analysis software. The size and shape of the ceftriaxone-conjugated and unconjugated biogenic AgNPs were characterized by transmission electron microscopy (TEM: G2 FEI, Netherlands) at the accelerating voltage of 200 kV (Muthu and Priya 2017; Dutta et al. 2017).

### Antimicrobial activity assay

The antimicrobial activity of the biogenic AgNPs was tested using well disc diffusion method (Baüer et al. 1966; MubarakAli et al. 2015). The experiment was tested against reference gram-positive (*Bacillus cereus* MTCC 1305, *S. aureus* MTCC 3160) and gram-negative bacteria (*Klebsiella pneumoniae* MTCC 3384, *Pseudomonas aeruginosa* MTCC 2453) procured from Microbial Type Culture Collection (MTCC), Chandigarh, India. An inoculum size of $10^5$ cells/mL was used to spread on the Mueller-Hinton Agar (MHA, HiMedia, India). Briefly, 20 mL of MHA was poured into petri dishes and allowed to solidify and 6-mm sterile discs were then placed appropriately. Finally, 50 μL (50 μg/mL) of colloidal AgNPs was loaded on each disc and sterile distilled water was used as a negative control. All the plates were incubated at 37 °C for 24 h. Diameters (mm) of cleared zones of inhibition (mm) formed around the discs were measured. All the assays were performed in triplicates under the same set of conditions for reproducibility (Ramkumar et al. 2017).

### MTT cytotoxicity assay

EAC cells were cultured in a 96-well plate at the density of $1 \times 10^8$ cells in 100 μL media/well with growth medium RPMI (Roswell Park Memorial Institute) supplemented with 10% FBS. Various concentrations of AgNPs (25, 50, 75, 100, and 200 μg $mL^{-1}$) were added to the cells and incubated for 24 h at 37 °C with $CO_2$ (5%) supplemented by a $CO_2$ incubator. After incubation, media were replaced with a fresh medium along with 20 μL of MTT (3-(4,5-dimethylthiazol-2-yl)-2,5-diphenyltetrazolium bromide) reagent and again incubated for 4 h at the same condition (Jeyaraj et al. 2013). A purple precipitate formed was visualized under inverted microscope, and then the medium was removed and 200 μL of 0.1% 0.1 N acidic isopropyl alcohol was added to each well. To dissolve the MTT formazan crystals, the plates were kept in the dark at 18–24 °C for overnight. After incubation, the absorbances were measured using a 96-well microplate reader (BioTek, Winooski, VT, USA) at 570 nm. Decreased cell viability upon AgNP treatment was calculated. $IC_{50}$ value was extrapolated from the plot of viability vs concentration. The percentage of growth inhibition was calculated using the following formula.

$$\text{Percentage of growth inhibition} = \frac{\text{Control OD–Treated OD}}{\text{Control OD}} \times 100$$

## Results and discussion

### Synthesis and spectral analysis of AgNPs and conjugates

The synthesis of AgNPs was achieved after the addition of *D. carota* extract. It was confirmed by UV-Vis Spectra gauzed from 200 to 800 nm. The generation of AgNPs with monodispersed stable nanoparticles by observing the SPR showed the maxima of 450 nm (Fig. 2). AgNPs have been established as a viable alternative for the development of novel antimicrobial agents and possess versatile applications as wound dressings and implant coatings as well as in the textile industry (Logeswari et al. 2013). Depending on the stated fact,

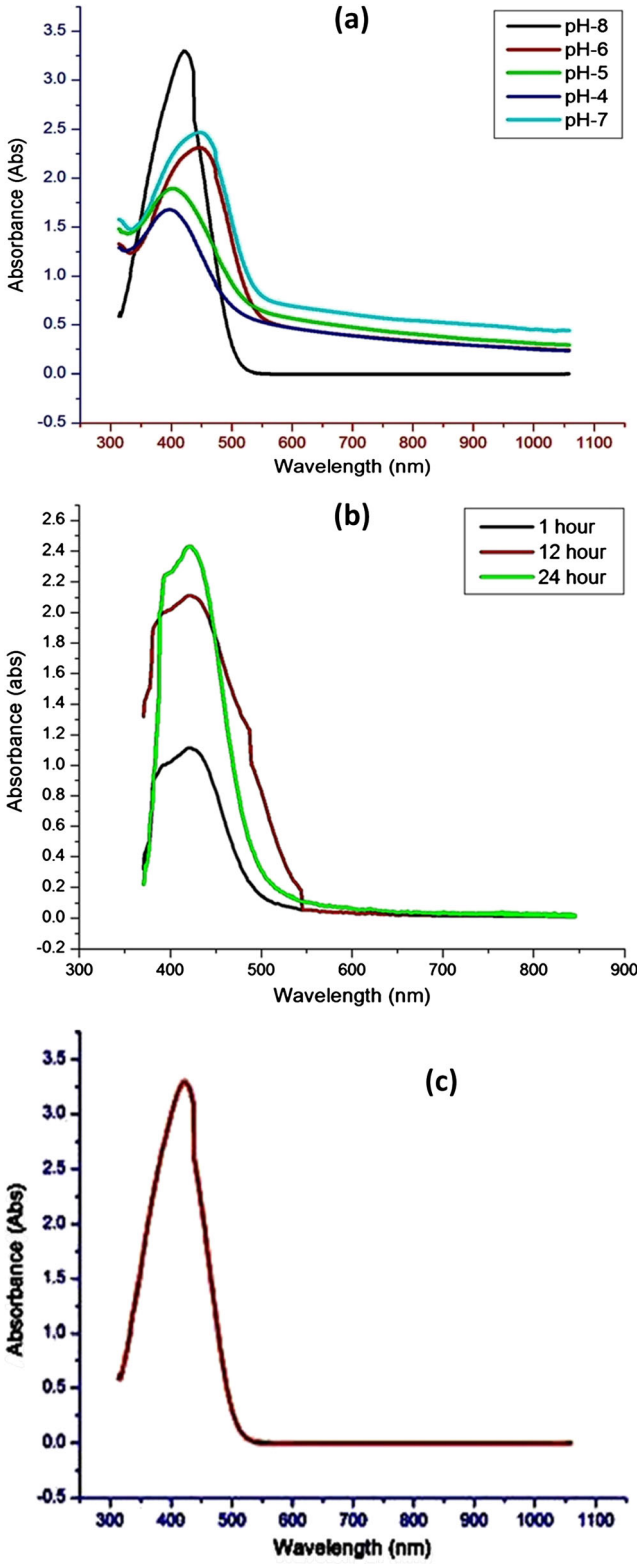


**Fig. 2** UV-visible spectra of plant extract-mediated biogenic AgNPs: by varying the conditions, pH (**a**); incubation time (**b**); biogenic AgNPs conjugated with antibiotics, ceftriaxone (**c**)

here a detailed study is reported on the biosynthesis of AgNPs, where $AgNO_3$ was reduced to AgNPs upon addition to *D. carota* extract. The formation of AgNPs was confirmed by the change in color of the solution from orange to dark brown. AgNPs have free electrons producing a surface plasmon resonance (SPR) band. Moreover, few significant parameters such as temperature, pH, and reaction time inferred a quantifiable influence on the absorbance and position of the SPR band (Suman et al. 2013; Kanmani and Lim 2013). The synthesis of AgNPs under different environmental conditions was further subjected to UV-spectral analysis. The synthesis was found to be the best after 24 h of the reaction at pH 8 and 30 °C (Fig. 2a, b). The absorption spectra of the conjugated AgNPs revealed the absorbance peak at 420 nm (Fig. 2c), which is the characteristic of the AgNPs (Singh et al. 2014).

Notable peaks were evident at 3389, 2099, 1399, and 1123 $cm^{-1}$ in the FT-IR spectra of *D. carota* extract (Fig. 3). These peaks could be assigned to N–H stretch, C=N stretch, $CH_3$ symmetry deformation, and aliphatic C=O stretch, respectively. The NH deformations, CN stretching, and CH deformation of vitamin C might also be responsible for the peaks observed at 1570 and 704 $cm^{-1}$, respectively (Yohannan Panicker et al. 2006). Hence, vitamin C (ascorbic acid) in the carrot extract could be an apparent capping or stabilizing agent for AgNPs. Moreover, the more prominent vibrational mode observed at 2109 and 1525 $cm^{-1}$ in AgNPs might be due to CN stretching and NO stretch mode (Christy and Umadevi 2012). The spectrum shows that absorption peaks of plain carrot extract was shifted when compared with the AgNPs due to the reduction of silver ions to AgNPs.

It is well known that the protein can bind to AgNPs through free amide groups (Lok et al. 2006; Sarkar et al. 2007). The IR spectrum results showed that the amide linkage of the protein had the stronger ability to bind silver so that the protein could form a coat covering around AgNPs, and it stabilized the aqueous medium. This evidence suggests that the biomolecules present in the extract of *D. carota* could possibly

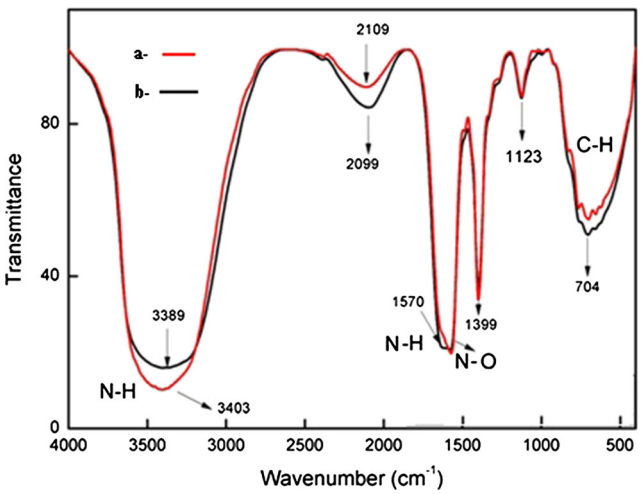


**Fig. 3** FT-IR analysis of biogenic AgNPs using extract of *D. carota* (**a**); biogenic AgNPs conjugated with ceftriaxone (**b**)

perform the formation of stable AgNPs. High negative zeta potential of AgNPs due to capping with negatively charged proteins may be the reason for stabilization of AgNPs. The bonding between ceftriaxone and AgNPs is still unclear. However, it is hypothesized that the amide group of ceftriaxone formed a strong bond towards AgNPs.

### Cystallinity and stability of AgNPs

Figure 4a shows the XRD pattern of the conjugated AgNPs. The XRD patterns of the AgNPs synthesized using ceftriaxone exhibited major sharp planes in the diffractogram, which indicated that the AgNPs were crystalline in nature. The planes at 38°, 44°, 64°, and 77° revealed the face-centered cubic (fcc) structure. The discernible planes could be indexed to (111), (200), (220), and (311) planes of a cubic unit cell, which corresponded to the cubic structure of AgNPs (JCPDS card No. 65-2871). This result correlated well with the previous studies reporting the synthesis of AgNPs using plant extracts (Gopinath et al. 2012; Jeyaraj et al. 2013). Crystalline size of conjugated AgNPs was calculated by following Scherrer's equation,

$$D = k\lambda/\beta\cos\theta$$

where

- $d$ mean crystallite size
- $k$ crystallite size (Å) taken as 0.89
- $\lambda$ wavelength of the incident beam
- $\beta$ full width at half maximum
- $\theta$ Bragg angle

The spectra revealed that the conjugated AgNPs showed a well crystalline structure of size, at 25 nm. In addition, some unassigned planes were also observed suggesting that the crystallization of some bioorganic phase occurred on the surface of the nanoparticles. Hence, it is clear that conjugated AgNPs were essentially crystalline. The AgNP solution showed polydispersed sizes ranging from 50 to 160 nm (Fig. 4b). Based on the hydrodynamic radii of the nanoparticles, particle size was determined to be high (Sahana et al. 2014).

### Topography and structural analysis of AgNPs

The crystalline structure and size of AgNPs were further characterized by TEM. The biologically synthesized AgNPs using the extract of *D. carota* and their structural morphology and crystallinity were further confirmed, in which shape and size of the AgNPs were investigated by adopting TEM analysis (Fig. 5). The aliquot of AgNPs was placed onto a drop-coated copper grid and allowed to dry. TEM images were recorded at different magnifications to find the individual particles. The AgNPs conjugated with ceftriaxone showed polydispersed spherical shaped nanoparticles (Fig. 5a, b). TEM images of bare AgNPs showed spherical shaped nanostructures with the particle size around 20 nm (Fig. 5c). However, variations observed in the particle sizes such as, 15, 25, 30, and 60 nm might be possibly due to the fact that the nanoparticles were being formed at different times (Sangwoo et al. 2016; Rajakumar and Abdul Rahuman 2011).

The topography and atomic arrangement of the biogenic AgNPs conjugated with ceftriaxone were characterized by the AFM images (Fig. 5d). The polydispersed AgNPs with ceftriaxone showed spherical shaped discrete particles with smooth surfaces without aggregation. Insight images showed the particle sizes of less than 100 nm using SPM lab analysis software. The topographical images of irregular AgNPs have also been documented, where it was clearly shown that apart from the nanoisland formation, there was also an agglomeration of silver. The particle size of the AgNPs was less than 100 nm and could be controlled by varying the synthesis conditions. The fabricated AgNPs were imaged by AFM to understand the exact configuration of the fabricated AgNPs and to confirm that the AgNPs were more or less homogenous in size and spherical in shape. The particle sizes

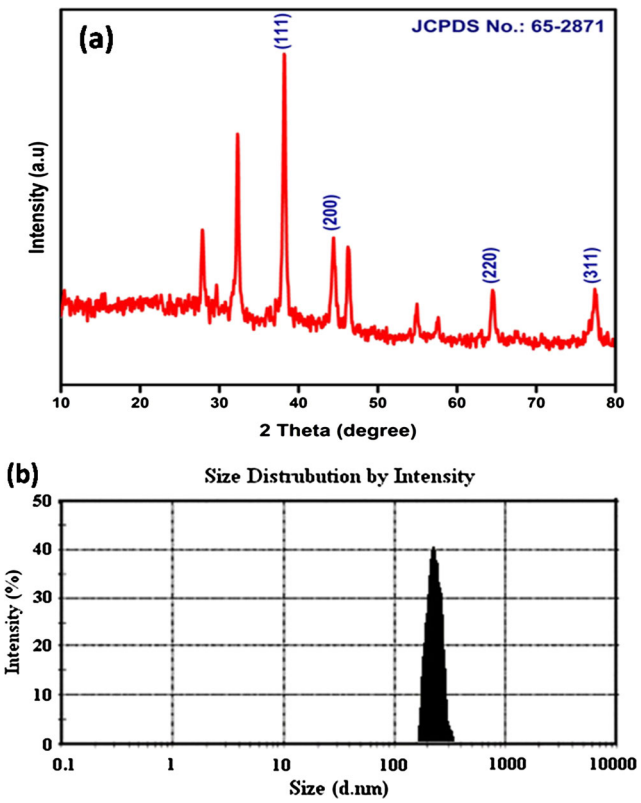


**Fig. 4** XRD patterns of ceftriaxone-conjugated AgNPs (**a**); zeta potential (**b**) showing the crystallinity of the AgNPs at (111), (200), and (220) and their size distribution up to 40%, respectively

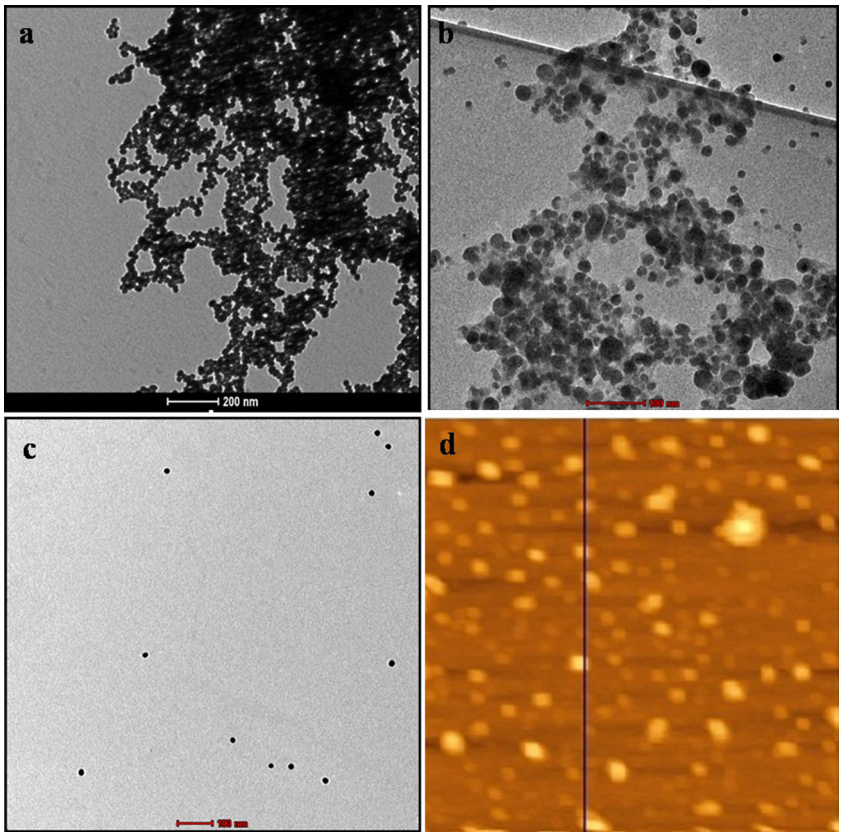


**Fig. 5** TEM images of biogenic AgNPs conjugated with ceftriaxone at different magnifications (**a**, **b**) and (**c**) indicates bare AgNPs before conjugation; AFM image, biogenic AgNPs conjugated with ceftriaxone (**d**)

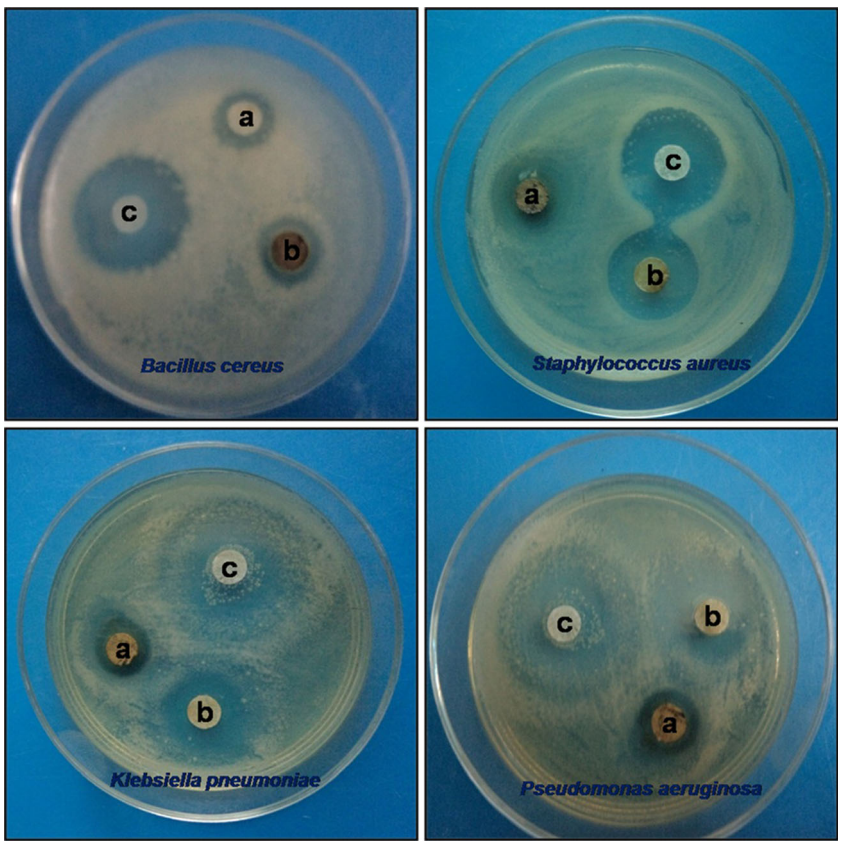


**Fig. 6** Antimicrobial activities of unconjugated AgNPs (**a**); ceftriaxone (**b**) and biogenic AgNPs conjugated with ceftriaxone (**c**) against *B. cereus* (*a*); *S. aureus* (*b*); *K. pneumoniae* (*c*); *P. aeruginosa* (*d*)

were measured using line profile determination of individual particles in the range of 20 nm.

### Antimicrobial activity of AgNPs and conjugates

The antibacterial activity of the biogenic AgNPs conjugated with ceftriaxone was tested against human pathogens, namely, *B. cereus*, *S. aureus*, *K. pneumoniae*, and *P. aeruginosa* by Kirby-Bauer disc diffusion assay (Fig. 6). The rationale behind selecting these two pathogens lies on their resistance against ceftriaxone antibiotic. In this study, the highest antimicrobial activity of AgNPs observed against *B. cereus* was 9 mm, whereas biogenic AgNPs conjugated with ceftriaxone (50 μg/mL) showed 21 mm (Fig. 6a). However, antimicrobial activity of AgNPs observed against *S. aureus* was 18 mm, whereas biogenic AgNPs conjugated with ceftriaxone (50 μg/mL) showed 23 mm (Fig. 6b). The lowest antimicrobial activity of AgNPs against *K. pneumoniae* was 10 mm whereas biogenic AgNPs conjugated with ceftriaxone showed 20 mm (Fig. 6c). The lowest antimicrobial activity of AgNPs against *P. aeruginosa* was 8 mm whereas biogenic AgNPs conjugated with ceftriaxone showed 18 mm (Fig. 6d). The test pathogens, which are in general resistant to ceftriaxone, were found to be more susceptible to AgNPs particularly to biogenic AgNPs conjugated with ceftriaxone. Hence, the application of ceftriaxone-conjugated nanoparticles is suggested as an alternative choice for the inhibition of the aforementioned pathogens (Harshiny et al. 2015).

The cell wall of Gram-positive bacteria is composed of a thick peptidoglycan layer, which consists of linear polysaccharide chains cross-linked by short peptides, thus forming a more rigid structure leading to difficult penetration of the AgNPs compared to the Gram-negative bacteria, where the cell wall possesses thinner peptidoglycan layers (Shrivastava et al. 2007; Gopinath et al. 2015). The enhanced antibacterial effects of novel AgNPs were witnessed and was also inferred that once inside the cell, the nanoparticles would interfere with the bacterial growth signaling pathway by modulating tyrosine phosphorylation of putative peptide substrates, critical for cell viability and division, and the nanoparticles were not in direct contact even within the aggregates, indicating stabilization of the nanoparticles by a capping agent (Shrivastava et al. 2007; Durán et al. 2005). The oligodynamic effect of silver has antibacterial activity against microorganisms. The changes in the local electronic structure on the surface of the smaller-sized particles have led to the enhancement of their chemical reactivities, leading to bactericidal effects (Thiel et al. 2007).

It was suggested that the direct usage of the AgNPs from the native reaction solution warranted more effective activities (Sondi and Salopek-Sondi 2004). Many theories exist, which explain the actions of the biogenic AgNPs that include altering the cell membrane structure, release of lipopolysaccharides and other membrane proteins, and lowering or increasing osmotic pressure due to accumulation or release of free radicals. However, the actual mechanism of the biogenic AgNPs conjugated with ceftriaxone is still unclear in this study. Thus, the need for evaluation of the precise mechanism of action of biogenic AgNPs conjugated with ceftriaxone prevails, which when uncovered might potentially rise to annihilate multidrug-resistant strains, emerging in recent times.

### Biocompatibility of AgNPs and conjugates

Despite its potent antibacterial activity and wide biological applications, the use of AgNPs as therapeutic agent is limited due to their potential for cytotoxic activity against mammalian cells (Mohanty et al. 2012). In this study, the cytotoxicity of biogenic AgNPs was tested against EAC cells using MTT assay, which relies on the fact that metabolically active cells reduce MTT to purple formazan. Hence, the intensity of the dye read at 570 nm was directly proportional to the number of viable cells. AgNPs exerted no significant cytotoxic effects at 50 μg/mL concentration (Fig. 7), which was found to be lethal for the bacteria tested in this study, indicating that the biogenic AgNPs were able to display antibacterial activity without being harmful to EAC cells at this concentration. Treatment at an

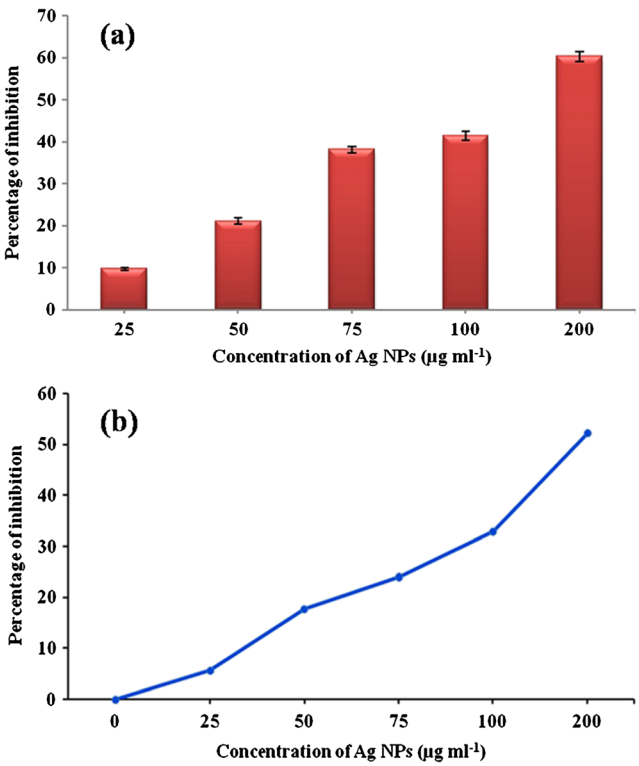


**Fig. 7** In vitro cytotoxicity effect of synthesized AgNPs on EAC cell lines showing non-toxicity observed from concentrations of 25, 50, and 75 μg/mL of AgNP treatment (**a**); $LD_{50}$ of AgNPs was determined at 200 μg/mL; cell viability percentage of AgNPs at various concentrations of AgNPs (**b**)

increasing dose of 75 μg/mL AgNPs resulted in approximately 40% reduction in cell viability (Fig. 7a). However, the higher dose 200 μg/mL led to the cells losing approximately 60% of viability (Fig. 7b). Earlier studies reported the in vitro cytotoxic property of AgNPs synthesized from *Piper longum* plant extract against Hep-2 cancer cell lines wherein 49% viability was observed at 31.25 μg/mL concentration of AgNPs (Jacob et al. 2012). It was also reported that AgNPs showed dose-dependent toxicity on Hep-2 cells (Gopinath et al. 2015). The specific reason and mechanism for dose-dependent cytotoxicity of AgNPs against EAC cells at higher concentrations need to be studied in detail.

## Conclusion

In this report, *D. carota* was used for the synthesis of AgNPs and subsequently a direct conjugation of AgNPs was performed with ceftriaxone. The presence of AgNPs and ceftriaxone-conjugated AgNPs was displayed by UV-Vis spectroscopy and AFM. The chemical association and stability of the nanosized particles were confirmed by FTIR and particle size analysis. The average size of biogenic AgNPs was 20 nm, and the size of the AgNPs conjugated with ceftriaxone was found to be less than 100 nm by TEM analysis. Further, the antimicrobial activities of the conjugated and the unconjugated AgNPs (50 μg/mL) against test pathogens were 23 and 18 mm against *S. aureus*, and 20 and 10 mm against *K. pneumoniae*, respectively. Thus, ceftriaxone showed increased efficacy due to the conjugation of AgNPs. Biogenic AgNPs (50 μg/mL) were observed to be biocompatible with to EAC cells. Thus, the as-prepared biogenic AgNps would pave way for the effective treatment of ceftriaxone-resistant pathogens and thus better management of ceftriaxone.

**Acknowledgements** The authors would like to acknowledge DST-FIST for providing the instrumentation facilities for characterization studies. Department of Biotechnology (DBT, Govt. Of India) is gratefully acknowledged for NRMC-F.

## References

Baüer AW, Kirby WM, Sherris JC, Turck M (1966) Antibiotic susceptibility testing by a standardized single disk method. J Clin Pathol 45: 493–496

Christy AJ, Umadevi M (2012) Synthesis and characterization of monodispersed silver nanoparticles. Adv Nat Sci Nanosci Nanotechnol 3:035013

Durán N, Marcato PD, Alves OL et al (2005) Mechanistic aspects of biosynthesis of silver nanoparticles by several *Fusarium oxysporum* strains. J Nanobiotechnol 3:8

Dutta PP, Bordoloi M, Gogoi K et al (2017) Antimalarial silver and gold nanoparticles: green synthesis, characterization and in vitro study. Biomed Pharmacother 91:567–580

Gomaa EZ (2017) Antimicrobial, antioxidant and antitumor activities of silver nanoparticles synthesized by *Allium cepa* extract: a green approach. J Genet Eng Biotechnol. doi:10.1016/j.jgeb.2016.12.002

Gopinath V, MubarakAli D, Priyadarshini S, Meera Priyadharsshini S, Thajuddin N, Velusamy P (2012) Biosynthesis of silver nanoparticles from *Tribulus terrestris* and its antimicrobial activity: a novel biological approach. Colloids Surf B: Biointerfaces 96:69–74

Gopinath V, Priyadarshini S, Loke MF et al (2015) Biogenic synthesis, characterization of antibacterial silver nanoparticles and its cell cytotoxicity. Arab J Chem. doi:10.1016/j.arabjc.2015.11.011

Harshiny M, Matheswaran M, Arthanareeswaran G et al (2015) Enhancement of antibacterial properties of silver nanoparticles–ceftriaxone conjugate through *Mukia maderaspatana* leaf extract mediated synthesis. Ecotoxicol Environ Saf 121:135–141

Iravani S, Korbekandi H, Mirmohammadi SV, Zolfaghari B (2014) Synthesis of silver nanoparticles: chemical, physical and biological methods. Res Pharm Sci 9:385–406

Jacob SJP, Finub JS, Narayanan A (2012) Synthesis of silver nanoparticles using *Piper longum* leaf extracts and its cytotoxic activity against Hep-2 cell line. Colloids Surf B Biointerfaces 91:212–214

Jeyaraj M, Sathishkumar G, Sivanandhan G, MubarakAli D et al (2013) Biogenic silver nanoparticles for cancer treatment: an experimental report. Colloids Surf B Biointerfaces 106:86–92

Kanmani P, Lim ST (2013) Synthesis and structural characterization of silver nanoparticles using bacterial exopolysaccharide and its antimicrobial activity against food and multidrug resistant pathogens. Process Biochem 48:1099–1106

Liu L, Yang J, Xie J et al (2013) The potent antimicrobial properties of cell penetrating peptide-conjugated silver nanoparticles with excellent selectivity for gram-positive bacteria over erythrocytes. Nano 5: 3834–3840

Logeswari P, Silambarasan S, Abraham J (2013) Ecofriendly synthesis of silver nanoparticles from commercially available plant powders and their antibacterial properties. Scientia Iranica 20:1049–1054

Lok C-N, Ho C-M, Chen R et al (2006) Proteomic analysis of the mode of antibacterial action of silver nanoparticles. J Proteome Res 5:916–924

Maráková N, Humpolíček P, Kašpárková V et al (2017) Antimicrobial activity and cytotoxicity of cotton fabric coated with conducting polymers, polyaniline or polypyrrole, and with deposited silver nanoparticles. Appl Surf Sci 396:169–176

Mohanty S, Mishra S, Jena P et al (2012) An investigation on the antibacterial, cytotoxic, and antibiofilm efficacy of starch-stabilized silver nanoparticles. Nanomed Nanotech Biol Med 8:916–924

MubarakAli D, Thajuddin N, Jeganathan K, Gunasekaran M (2011) Plant extract mediated synthesis of silver and gold nanoparticles and its antibacterial activity against clinically isolated pathogens. Colloids Surf B Biointerfaces 85:360–365

MubarakAli D, Sang-Yul L, Seong-Cheol K, Jung-Wan K (2015) One-step synthesis of cellulose/silver nanobiocomposites using a solution plasma process and characterization of their broad spectrum antimicrobial efficacy. RSC Adv 5:35052–35060

MubarakAli D, Seong-Cheol K, Sang-Yul L, Jung-Wan K (2016) The facile synthesis of chitosan-based silver nano-biocomposites via a solution plasma process and their potential antimicrobial efficacy. Arch Biochem Biophys 605:49–58

Muthu K, Priya S (2017) Green synthesis, characterization and catalytic activity of silver nanoparticles using *Cassia auriculata* flower extract separated fraction. Spectrochim Acta Mol Biomol Spectrosc 179:66–72

Ostaszewska T, Chojnacki M, Kamaszewski M, Sawosz-Chwalibóg E (2016) Histopathological effects of silver and copper nanoparticles on the epidermis, gills, and liver of Siberian sturgeon. Environ Sci Pollut Res Int 23:1621–1633

Pugazhendhi S, Kirubha E, Palanisamy PK, Gopalakrishnan R (2015) Synthesis and characterization of silver nanoparticles from *Alpinia*

*calcarata* by Green approach and its applications in bactericidal and nonlinear optics. Appl Surf Sci 357:1801–1808

Pugazhendhi S, Sathya P, Palanisamy PK, Gopalakrishnan R (2016) Synthesis of silver nanoparticles through green approach using *Dioscorea alata* and their characterization on antibacterial activities and optical limiting behavior. J Photochem Photobiol B 159:155–160

Rajakumar G, Abdul Rahuman A (2011) Larvicidal activity of synthesized silver nanoparticles using *Eclipta prostrata* leaf extract against filariasis and malaria vectors. Acta Trop 118:196–203

Ramkumar VS, Pugazhendhi A, Gopalakrishnan K et al (2017) Biofabrication and characterization of silver nanoparticles using aqueous extract of seaweed *Enteromorpha compressa* and its biomedical properties. Biotechnol Rep 14:1–7

Sahana R, Daniel SCGK, Sankar SG et al (2014) Formulation of bactericidal cold cream against clinical pathogens using *Cassia auriculata* flower extract-synthesized Ag nanoparticles. Green Chem Lett Rev 7:64–72

Salem JK, El-Nahhal IM, Najri BA et al (2016) Effect of anionic surfactants on the surface plasmon resonance band of silver nanoparticles: determination of critical micelle concentration. J Mol Liq 223:771–774

Sangwoo N, MubarakAli D, Jungwan K (2016) Characterization of alginate/silver nanobiocomposites synthesized by solution plasma process and their antimicrobial properties. J Nanomater 4712813:9

Saratale GD, Saratale RG, Benelli G et al (2017) Anti-diabetic potential of silver nanoparticles synthesized with *Argyreia nervosa* leaf extract high synergistic antibacterial activity with standard antibiotics against foodborne bacteria. J Clust Sci 28:1709–1727

Sarkar S, Jana AD, Samanta SK, Mostafa G (2007) Facile synthesis of silver nano particles with highly efficient anti-microbial property. Polyhedron 26:4419–4426

Shankar PD, Shobana S, Karuppusamy I et al (2016) A review on the biosynthesis of metallic nanoparticles (gold and silver) using bio-components of microalgae: formation mechanism and applications. Enzym Microb Technol 95:28–44

Shrivastava S, Bera T, Roy A et al (2007) Characterization of enhanced antibacterial effects of novel silver nanoparticles. Nanotechnology 18:225103

Singh D, Rathod V, Ninganagouda S et al (2014) Optimization and characterization of silver nanoparticle by endophytic fungi *Penicillium* sp. isolated from *Curcuma longa* (turmeric) and application studies against MDR *E. coli* and *S. aureus*. Bioinorg Chem Appl 2014: e408021

Sondi I, Salopek-Sondi B (2004) Silver nanoparticles as antimicrobial agent: a case study on *E. coli* as a model for gram-negative bacteria. J Colloid Interface Sci 275:177–182

Sperling RA, Parak WJ (2010) Surface modification, functionalization and bioconjugation of colloidal inorganic nanoparticles. Philos Trans R Soc Lond A 368:1333–1383

Su Y, Zhao L, Meng F et al (2017) Silver nanoparticles decorated lipase-sensitive polyurethane micelles for on-demand release of silver nanoparticles. Colloids Surf B: Biointerfaces 152:238–244

Suman TY, Radhika Rajasree SR, Kanchana A, Elizabeth SB (2013) Biosynthesis, characterization and cytotoxic effect of plant mediated silver nanoparticles using *Morinda citrifolia* root extract. Colloids Surf B: Biointerfaces 106:74–78

Thiel J, Pakstis L, Buzby S et al (2007) Antibacterial properties of silver-doped titania. Small 3:799–803

Venugopal K, Rather HA, Rajagopal K et al (2017) Synthesis of silver nanoparticles (Ag NPs) for anticancer activities (MCF 7 breast and A549 lung cell lines) of the crude extract of *Syzygium aromaticum*. J Photochem Photobiol B Biol 167:282–289

Vijayan SR, Santhiyagu P, Ramasamy R et al (2016) Seaweeds: a resource for marine bionanotechnology. Enzym Microb Technol 95: 45–57

Yohannan Panicker C, Tresa Varghese H, Philip D (2006) FT-IR, FT-Raman and SERS spectra of vitamin C. Spectrochim Acta Mol Biomol Spectrosc 65:802–804